Inactivation of Myosin Binding Protein C Homolog in Zebrafish as a Model for Human Cardiac Hypertrophy and Diastolic Dysfunction

Yau-Hung Chen, Chiung-Wen Pai, Shu-Wei Huang, Sheng-Nan Chang, Lian-Yu Lin, Fu-Tien Chiang, Jiunn-Lee Lin, Juey-Jen Hwang and Chia-Ti Tsai

J Am Heart Assoc. 2013;2:e000231; originally published September 18, 2013;
doi: 10.1161/JAHA.113.000231
The *Journal of the American Heart Association* is published by the American Heart Association, 7272 Greenville Avenue, Dallas, TX 75231
Online ISSN: 2047-9980

ORIGINAL RESEARCH

Inactivation of Myosin Binding Protein C Homolog in Zebrafish as a Model for Human Cardiac Hypertrophy and Diastolic Dysfunction

Yau-Hung Chen, PhD; Chiung-Wen Pai, MS; Shu-Wei Huang, MS; Sheng-Nan Chang, MD; Lian-Yu Lin, MD, PhD; Fu-Tien Chiang, MD, PhD; Jiunn-Lee Lin, MD, PhD; Juey-Jen Hwang, MD, PhD; Chia-Ti Tsai, MD, PhD

***Background*—**Sudden cardiac death due to malignant ventricular arrhythmia is a devastating manifestation of cardiac hypertrophy. Sarcomere protein myosin binding protein C is functionally related to cardiac diastolic function and hypertrophy. Zebrafish is a better model to study human electrophysiology and arrhythmia than rodents because of the electrophysiological characteristics similar to those of humans.

***Methods and Results*—**We established a zebrafish model of cardiac hypertrophy and diastolic dysfunction by genetic knockdown of myosin binding protein C gene (*mybpc3*) and investigated the electrophysiological phenotypes in this model. We found expression of zebrafish *mybpc3* restrictively in the heart and slow muscle, and *mybpc3* gene was evolutionally conservative with sequence homology between zebrafish and human *mybpc3* genes. Zebrafish with genetic knockdown of *mybpc3* by morpholino showed ventricular hypertrophy with increased myocardial wall thickness and diastolic heart failure, manifesting as decreased ventricular diastolic relaxation velocity, pericardial effusion, and dilatation of the atrium. In terms of electrophysiological phenotypes, *mybpc3* knockdown fish had a longer ventricular action potential duration and slower ventricular diastolic calcium reuptake, both of which are typical electrophysiological features in human cardiac hypertrophy and heart failure. Impaired calcium reuptake resulted in increased susceptibility to calcium transient alternans and action potential duration alternans, which have been proved to be central to the genesis of malignant ventricular fibrillation and a sensitive marker of sudden cardiac death.

Conclusions*—mybpc3* knockdown in zebrafish recapitulated the morphological, mechanical, and electrophysiological phenotypes of human cardiac hypertrophy and diastolic heart failure. Our study also first demonstrated arrhythmogenic cardiac alternans in cardiac hypertrophy. **(*J Am Heart Assoc.* 2013;2:e000231 doi: 10.1161/JAHA.113.000231)**

Key Words: animal model • cardiac alternans • diastolic dysfunction • heart failure with normal ejection fraction • hypertrophy • zebrafish

The myosin binding protein C (MYBPC) gene (*mybpc3*) encodes myosin binding protein C, a key constituent of the thick filaments localized to doublets in the C-zone of the A-band of the sarcomere. By binding to myosin, titin, and actin, MYBPC contributes to maintaining the structural integrity of the sarcomere and regulates cardiac contractility and relaxation.[1–4] Mutations of *mybpc3* gene have been demonstrated to be associated with a risk of cardiac hypertrophy and represent one of the common causes of hypertrophic cardiomyopathy.[2–4] Recently, it has also been demonstrated that genetic variants in human *mybpc3* gene are associated with susceptibility to diastolic heart failure without overt cardiac hypertrophy.[5] Therefore, the function of MYBPC is closely related to cardiac structural and function and may be a new therapeutic target in the treatment of cardiac hypertrophy and diastolic dysfunction.

Diastolic heart failure or heart failure with a normal ejection fraction (HFNEF) is one of the most important and common cardiovascular diseases. Clinically, the most common cause of diastolic heart failure is left ventricular hypertrophy, resulting either primarily from hypertrophic cardiomyopathy or secondarily from hypertension and aortic

From the Department of Chemistry (Y.-H.C.), Tamkang University, Taipei, Taiwan; Department of Life Sciences and Institute of Genome Sciences (C.-W.P.), National Yang-Ming University, Taipei, Taiwan; Department of Internal Medicine (S.-N.C., C.-T.T.), National Taiwan University Hospital Yun-Lin Branch, Yun-Lin, Taiwan; Division of Cardiology (S.-W.H., L.-Y.L., F.-T.C., J.-L.L., J.-J.H., C.-T.T.), Department of Internal Medicine, National Taiwan University College of Medicine and Hospital, Taipei and Yun-Lin, Taiwan; and Department of Laboratory Medicine (F.-T.C.), National Taiwan University Hospital, Taipei, Taiwan.

Correspondence to: Chia-Ti Tsai, MD, PhD, Division of Cardiology, Department of Internal Medicine, National Taiwan University College of Medicine and Hospital, No. 7, Chung-Shan South Road, Taipei 100, Taiwan. E-mail: cttsai@ntuh.gov.tw; cttsai1999@gmail.com

Received February 4, 2013; accepted July 30, 2013.

stenosis. One of the common causes of death in patients with left ventricular hypertrophy is malignant ventricular arrhythmia.[6,7] Sudden cardiac death (SCD) due to malignant ventricular arrhythmia is the most devastating manifestation of cardiovascular diseases. The Framingham Heart Study reported that left ventricular hypertrophy was associated with an increased risk of SCD in a community-based cohort.[7] Because the hemodynamic pathophysiology of cardiac hypertrophy is well known, the fundamental electrophysiological mechanism of SCD or malignant ventricular arrhythmia in cardiac hypertrophy is not completely understood.[8] Although there are several murine models of cardiac hypertrophy, such as genetic ablation of *mybpc3* or aortic banding in mice,[4,9] the electrophysiological phenotypes of murine hearts are completely different from those of human heart due to a very high heart rate and very short action potential duration (APD), which hinder the evaluation of cardiac repolarization.[10] Because the electrophysiological phenotypes of large animal heart are closer to those of human heart,[11] currently there has been no well-established model of cardiac hypertrophy or diastolic dysfunction in large animals.

Recently, zebrafish has been proved to be a good model in which to study human cardiac electrophysiology, especially cardiac repolarization, because its heart rate and action potential morphology strikingly resemble those of human heart.[10,12] Accordingly, in the present study, based on the role of MYBPC on cardiac hypertrophy and diastolic dysfunction,[2–5] we sought to establish a zebrafish model of human cardiac hypertrophy and diastolic heart failure by genetic knockdown of *mybpc3*. We first systematically characterized the status and expression pattern of *mybpc3* gene in zebrafish, which had never been reported before. Then we tried to recapitulate the structural, mechanical, and electrophysiological phenotypes of human cardiac hypertrophy and diastolic heart failure in this zebrafish model.

Methods

Cloning of Zebrafish *mybpc3* cDNA

For amplifying *mybpc3* cDNA, 3 primer sets [(Mybpc3-1 forward: 5′-ACACTCAACCAGGATGCCAG-3′ and Mybpc3-1 reverse: 5′-TCAGTGACGGTCTTCTCATCTC-3′), (Mybpc3-2 forward: 5′-TGGCTGAAGAATGGACAAGAGA-3′ and Mybpc3-2 reverse: 5′-TTCCTTGCAGTACTCAACACCA-3′), and (Mybpc3-3 forward: 5′-CTCCACCAGCGAGCCTATTG-3′ and Mybpc3-3 reverse: 5′-ACGTCTCTCTCATTTCTTGATGTCT-3′)] were designed according to an ensemble contig (ENSDART00000099789) and a National Center for Biotechnology Information sequence (NM_001044399) encoding of a putative zebrafish Mybpc3. According to reverse transcription–polymerase chain reaction (RT-PCR) experiments, 3 DNA fragments were amplified, subcloned, and sequenced.[13,14] The presumptive Mybpc3 amino acid sequences were determined using the Wisconsin Sequence Analysis Package v.10.0 (GCG). The Gap program of that package was used for pair comparisons, and the Pileup and Prettybox programs were used for multiple comparisons. The Clustalw molecular evolution genetic program was used for our phylogenic tree analysis (http://www.ebi.ac.uk/clustalw/).

Zebrafish Embryos, Whole Mount In Situ Hybridization, Antibody Labeling, and Cryosection

The procedures for zebrafish culture, embryo collection, fluorescent observation, whole mount in situ hybridization, antibody labeling, and cryosection have been described previously.[13–15] The designation of developmental stages of zebrafish followed those of Kimmel et al.[16] According to the guidelines of zebrafish anesthesia and euthanasia,[15] there is no evidence of higher order cognition in zebrafish during the first week of development. During the first week of development, embryonic movements are simple reflexes that do not provide evidence for a capacity for suffering. Thus, during the first week, zebrafish larvae have not reached the point in brain development where stimuli can be experienced as aversive.

Both *mybpc3* and *cmlc2* were used as probes.[17] They were digoxigenin labeled after their partial DNA fragments were cloned.

Preparation and Microinjection of Morpholino

Mybpc3-morpholino (MO) (5′-CTCTGGCATCCTGGTTGAGTGTCCC-3′; Gene Tools) was established according to zebrafish *mybpc3* cDNA sequence for blocking translation. Negative control MO (5′-CCTCTTACCTCAGTTACAATTTATA-3′) was designed according to the random nucleotide sequences. All of these were prepared at stocking concentrations of 1 mmol/L and diluted with double-distilled water to the proper concentrations (4.5 ng/2.3 nL).

Microscopic Observation of Zebrafish Embryos

All embryos were observed at specific stages under a microscope (DM 2500; Leica) equipped with Nomarski differential interference contrast optics and a fluorescent module with a GFP filter cube (Kramer Scientific). Photographs of embryos at specific stages were taken with a CCD (DFC490; Leica). Measurement of myocardial wall thickness in the embryo heart was performed as previously reported,[18] using a camera with high temporal (14 frames/s) and spatial (5184×3456 pixels) resolutions (Canon EOS-1DX).

Evaluation of In Vivo Systolic and Diastolic Functions of the Zebrafish Embryo Heart

We evaluated the systolic and diastolic functions in the zebrafish embryo heart using the automatic video edge-detection system.[19] In brief, SoftEdge (IonOptix Corporation) was used to measure real-time length via contrast analysis of digitized image data. Edge detection was based on image intensity, and image contrast was enhanced using the video gain and offset controls. The signal was calibrated using a standard millimeter graticule. The calculated values were verified by conventional velocity measurement obtained from 2-dimensional images using a camera with high temporal (14 frames/s) and spatial (5184×3456 pixels) resolutions (Canon EOS-1DX). Velocity values were expressed as micrometers per second for myocardial wall velocity in systole and diastole to represent the systolic and diastolic functions, respectively.

Extraction of Zebrafish Embryo Heart and In Vitro Electrophysiological Recordings

The heart of the embryo was dissected from the thorax en bloc by using fine forceps and then transferred to the recording chamber. Only spontaneously beating whole hearts were studied. All experiments were performed at room temperature. The recording chamber was superfused with solution containing (in mmol/L) NaCl 140, KCl 4, $CaCl_2$ 1.8, $MgCl_2$ 1, glucose 10, and HEPES 10, pH 7.4.[10] Action potentials were recorded by the microelectrode and disrupted patch method, as previously reported.[10] Action potentials were measured by using an amplifier (Axopatch 200B; Axon Instrument) and digitized with a 12-bit analog-to-digital converter (Digidata 1440A Interface; Molecular Devices). Resting action potentials were first recorded and then triggered by incrementally injecting pulses of depolarizing current. For calcium transient recording, the embryo hearts were stained with Fluo 3–acetoxymethyl ester (5 μmol/L; Molecular Probes) and then recorded with an inverted confocal microscope (LSM 510; Carl Zeiss) as previously recorded.[20] For fluorescence excitation, the 488-nm band of an argon laser was used. Emission was recorded using a long-pass LP 515 filter set.[20]

Measurement of APD and Calcium Transient Alternans and Calcium Transient Decay Rate

Alternans of APD (APD-ALT) and calcium transient (Ca-ALT) were determined by measuring differences in local APD and calcium transient amplitude on consecutive beats as previously reported.[21] The APD-ALT (in ms) and Ca-ALT (in %) were plotted against the pacing rates (PRs).

The calcium transient decay rate was measured as previously reported.[21,22] The calcium level was reported as F/F0, where F0 was the resting or diastolic fluorescence level. To quantify the calcium transient decay rate, the decay portion of the calcium transient (from 30% to 100% of decline phase) was fit to a single exponential function whose time constant, τ, was used to measure calcium transient decay rate.[22,23]

Statistical Methods

All data were expressed as mean±SD. Continued data from independent group were compared by using the Mann-Whitney *U* test. The Cochran-Armitage test was used to test a trend of the dose–response relationship between frequencies of phenotypic abnormalities and dose of Mybpc3-MO injection. A P value <0.05 was considered statistically significant.

Results

Cloning of Zebrafish *mybpc3* cDNA and Comparison of Deduced Amino Acid Sequences

In searching the GenBank database, we found 1 putative zebrafish *mybpc3* sequence (NM_001044349). After RT-PCR and DNA sequencing, we found there exist 3 *mybpc3* transcription variants (*mybpc3-tv1*, *-tv2*, and *-tv3*) during zebrafish early embryogenesis (Figure 1A). After sequence cross-comparison, we found there are 5 differences between human and zebrafish *mybpc3* transcripts (indicated by arrows 1 to 5). For example, all zebrafish *mybpc3* transcription variants lack the second exon (arrow 1) but possess 2 extra exons (arrows 3 and 5); zebrafish *mybpc3-tv2* and *-tv3* have an extra exon (arrows 4 and 2) in comparison with *mybpc3-tv1*.

The deduced zebrafish Mybpc3-tv1 amino acid sequence consists of a 1276–amino acid polypeptide. The zebrafish Mybpc3-tv1 polypeptide shares sequence identities of 63%, 61%, 62%, 63%, 61%, 68%, and 70% with the reported Mybpc3 of human, chimpanzee, bovine, mouse, rat, chicken, and *Xenopus*, respectively. We used the Clustalw program to determine the phylogenic similarities between zebrafish Mybpc3-tv1 and other known species. The phylogenic tree generated by the program showed that zebrafish Mybpc3-tv1 possesses a unique pattern, different from those of higher vertebrates (data not shown).

We therefore examed the expression profile of 3 individual *mybpc3* transcripts by the use of RT-PCR and found that *mybpc3-tv1* signals are detectable from 18 to 96 hours postfertilization (hpf) (except for 48 hpf); *mybpc3-tv2* signals are detectable at 18 to 48 hpf; and *mybpc3-tv3* signals are detectable at 48 to 96 hpf (Figure 1B). These observations suggest that these 3 zebrafish *mybpc3* transcripts have a unique profile during zebrafish early embryogenesis.

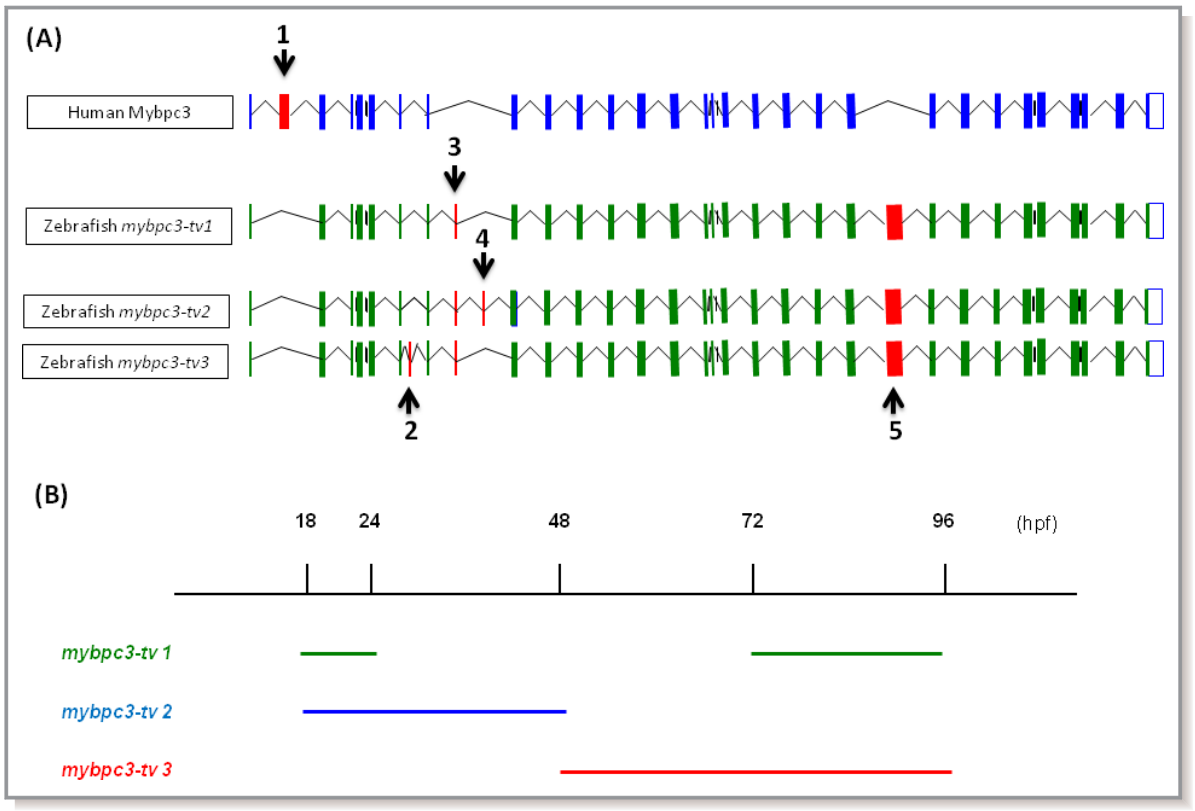

Figure 1. Gene structures and expression profiles of *mybpc3* during zebrafish early embryogenesis. A, Schematic illustration of human MYBPC3 gene and 3 zebrafish *mybpc3* transcripts. The differences between human and zebrafish mybpc3 are marked by the red box and arrows. B, Expression profiles of 3 zebrafish transcriptional variants (*mybpc3-tv1*, *-tv2*, and *-tv3*). hpf indicates hours postfertilization; MYBPC, myosin binding protein C; tv, transcription variant.

Zebrafish *mybpc3* Expressed in Heart and Slow Muscle

We next determined the overall expressions of 3 *mybpc3* mRNAs (combinations of *mybpc3-tv1*, *-tv2*, and *-tv3*) in zebrafish embryos by using whole mount in situ hybridization. During early embryonic development, *mybpc3* expressions first became evident in the developing somites and heart tube (Figure 2A and 2B). At later stages, *mybpc3* mRNA remained restricted to the heart and skeletal muscle throughout embryogenesis (Figure 2C and 2D). Cryosection results showed that *mybpc3* mRNAs expressions are restricted in the ventricle and slow muscle but faint in the atrium (Figure 2E through 2J).

Loss of *mybpc3* Leads to Cardiac Hypertrophy and Diastolic Heart Failure in Zebrafish

To investigate the role of MYBPC in vivo, we knocked zebrafish *mybpc3* down by injecting morpholino-modified antisense oligonucleotides directed against translational start site (Mybpc3-MO) into one-cell–stage zebrafish embryos. We found that negative control MO or Mybpc3-MO–injected embryos showed normal heart morphogenesis during the first 24 hours of development (24 hpf). By 72 hpf, Mybpc3-MO–injected zebrafish showed pericardial edema and enlarged cardiac chambers as determined in bright field imaging (Figure 3A and 3B), which recapitulated typical features of human heart failure. In human heart failure, edema often occurs in dependent parts, such as bilateral lower legs. In embryonic fish, the pericardiac sac is the dependent part, and heart failure usually manifests as pericardial edema.[10] The ventricular wall thickness was also increased in the Mybpc3-MO–injected zebrafish (diastolic wall thickness 15.1±0.8 μm in morphants and 13.4±0.7 μm in control embryos; P=0.009), resembling human ventricular hypertrophy. Immunostaining using both atrial and ventricular specific markers showed mild enlargement of the ventricle but significant enlargement of the atrium (Figure 3C and 3D), a typical feature of human diastolic dysfunction.[24,25] Histologically, the Mybpc3-MO–injected heart showed ventricular hypertrophy (Figure 3E and 3F). Finally, increased expression of sarcomere proteins has been used as a marker of cardiac hypertrophy.[26,27] Accordingly, we also found that Mybpc3-MO–injected hearts showed an increased expression of sarcomere protein, cardiac myosin light chain 2 (cmlc2), as determined with nonquantitative in situ hybridization (Figure 3G and 3H).

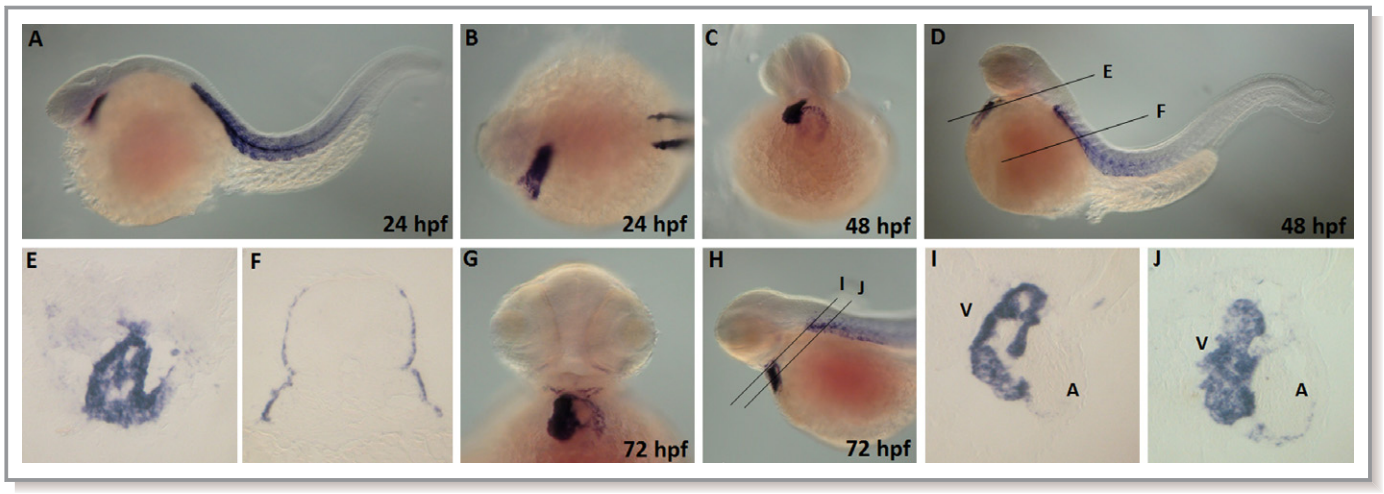

Figure 2. *mybpc3* expression patterns during zebrafish embryogenesis. A through D, Whole mount in situ hybridization of 24-hpf-, and 48-hpf-embryos shows that *mybpc3* expresses in heart and somites. E and F, Cryosectioning showed that the expressions *mybpc3* were restricted in ventricle, atrium, and slow muscles. G through J, By 72 hpf, *mybpc3* signals were still detectable in ventricle and atrium but were down-regulated in muscle. A indicates atrium; hpf, hours postfertilization; mybpc, myosin binding protein C; V, ventricle.

Interestingly, the frequencies of phenotypic abnormalities in consequence of Mybpc3-MO injection followed a dose-dependent manner (Table). At 2.0 ng, 36.1% (total cases in triplicate experiments, n=88) of the surviving embryos (n=244) displayed heart failure phenotypes, and at 3.0 ng, the percentage increased to 46.4% (n=116; Table) (P=0.011 for trend test).

We further characterized the alternation of mechanical function after loss of *mybpc3* function. The ventricular systolic functions were comparable between the negative control MO or Mybpc3-MO–injected embryos, as determined by measurement of maximal ventricular systolic velocity (226±64 μm/s in morphants and 214±52 μm/s in control embryos; P>0.05). However, Mybpc3-MO–injected embryos showed significantly impaired ventricular diastolic function, as determined by measurement of maximal ventricular diastolic relaxation velocity (213±58 μm/s in morphants and 297±65 μm/s in control embryos; P=0.043). These features resembled those of human heart failure with preserved left ventricular ejection fraction (HFNEF) or diastolic dysfunction.

Taken together, the Mybpc3-MO–injected fish showed typical features of human diastolic heart failure with dilated atrium, ventricular hypertrophy, and preserved ventricular systolic function.[24,25]

Mybpc3-MO–Injected Zebrafish Have a Longer APD and Increased Susceptibility to Arrhythmogenic APD-ALT

We then characterized the electrophysiological phenotypes after loss of *mybpc3* function. The action potentials of the zebrafish embryo hearts were recorded under in vitro conditions (Figure 4). The resting APD was longer in the Mybpc3-MO–injected heart, compared with that of the control fish heart (mean APD 316±31 ms versus 278±25 ms, P=0.007). Interestingly, prolonged APD is the pathognomic electrophysiological feature of human cardiac hypertrophy and heart failure.[28,29]

Recently, it has been demonstrated that repolarization or APD-ALT is central to genesis of malignant ventricular arrhythmia or ventricular fibrillation and is a highly sensitive marker of susceptibility to SCD.[30] We sought to investigate whether loss of *mybpc3* function led to increased susceptibility to APD-ALT. Incremental pacing was performed to evaluate the relationship between APD-ALT and PR in control and Mybpc3-MO–injected hearts (Figure 5). In Mybpc3-MO–injected hearts, there was a leftward shift in the APD-ALT–to–PR relationship (Figure 5B). In other words, at each PR, the magnitude of ALT was always greater in the Mybpc3-MO–injected hearts, indicating greater susceptibility to APD-ALT .[21] Therefore, in addition to ventricular hypertrophy and diastolic heart failure, Mybpc3-MO–injected hearts may be more susceptible to ventricular arrhythmia or fibrillation because of greater susceptibility to APD-ALT.

Mybpc3-MO–Injected Zebrafish Show Slower Diastolic Calcium Decay and Increased Susceptibility to Ca-ALT

Accumulating evidence has shown that APD-ALT arise primarily from Ca-ALT in both intact whole hearts[31] and in vitro cardiomyocytes.[21] In the next step, we tried to investigate the calcium dynamics in the Mybpc3-MO–injected hearts.

The calcium transient of the Mybpc3-MO–injected hearts showed characteristic features as seen in mammalian

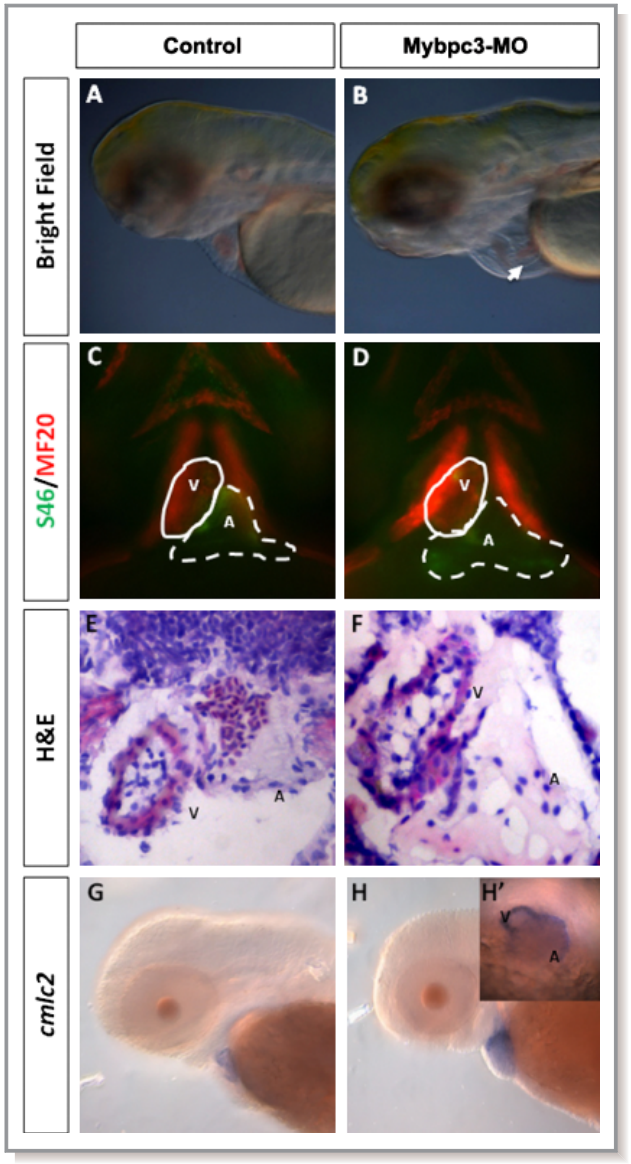

Figure 3. Knockdown of *mybpc3* in zebrafish embryos leads to cardiomyopathy. A and B, Morphology of the embryonic zebrafish heart (72 hpf) with Mybpc3-MO injection or control. Arrow indicates the position of atrium. C and D, Embryos derived from control or Mybpc3-MO–injected group were stained with different antibodies MF20 (red) and S46 (green), and results reveals that *Mybpc3* knockdown causes enlarged cardiac chambers, especially the atrium. Dashed and solid lines marked the morphology of atrium and ventricle, respectively. E and F, Hematoxylin and eosin (H&E) staining shows that *mybpc3*-morphants have ventricular hypertrophy and thinner atrial wall. G and H, Whole mount in situ hybridization using a cardiac-specific marker *cmlc2* as probes and showing that inactivation of *mybpc3* causes increased heart size. H′, Ventral view of H. A indicates atrium; hpf, hours postfertilization; MO, morpholino; mybpc, myosin binding protein C; V, ventricle.

hypertrophic and failure hearts.[29,32] The rising time was longer, and the peak calcium was smaller (Figure 6). The decay rate of calcium transient was also slower, with a larger time constant, indicating defective calcium reuptake and cycling.[21,23] Defective intracellular calcium cycling may directly contribute to Ca-ALT.[21,23,31] We then sought to investigate whether Mybpc3-MO–injected hearts also had increased susceptibility to Ca-ALT.

Incremental pacing was performed to evaluate the relationship between Ca-ALT and PR in control and Mybpc3-MO–injected hearts (Figure 7). Like in the study of APD-ALT, in Mybpc3-MO–injected hearts, there was a leftward shift in the Ca-ALT–to–PR relationship, indicating greater susceptibility to Ca-ALT. Interestingly, the developments of APD-ALT and Ca-ALT were closely related and coupled, and both are highly rate dependent.

In summary, the Mybpc3-MO–injected hearts showed characteristic electrophysiological features with greater susceptibility to arrhythmogenetic cardiac ALT as those seen in mammalian hypertrophic and failure heart.

Discussion

In the present study, we have systematically characterized the expression of *mybpc3* in zebrafish and demonstrated that loss of *mybpc3* in zebrafish recapitulates the morphological, mechanical, and electrophysiological phenotypes of human cardiac hypertrophy and diastolic heart failure. We have also first shown that *mybpc3* gene is evolutionally conservative and is an essential gene for the cardiac development of vertebrates, because loss of *mybpc3* leads to severe cardiac phenotypes. This is also the first study to demonstrate an increased susceptibility to arrhythmogenic cardiac ALT in a zebrafish model of cardiac hypertrophy and diastolic dysfunction.

In the characterization of *mybpc3* gene expression in zebrafish, we found sequence homology between human and zebrafish *mybpc3* genes. Furthermore, ablation of *mybpc3* gene expression results in similar phenotypes in zebrafish and human hearts. These results implicate that zebrafish heart is a feasible model system in which to dissect the detailed pathophysiological mechanism of human cardiovascular diseases. Previously, Norton et al[33] reported a similar approach to induce heart failure in zebrafish to study the function of BCL2-associated athanogene 3 gene in humans. However, in this study, only mechanical phenotypes were characterized. The most devastating phenotype of human heart failure is ventricular arrhythmia or SCD. Therefore, correlating the electrophysiological phenotype to mechanical phenotype is important and clinically relevant. Notably in the present study, we characterized both the mechanical and electrophysiological phenotypes in the zebrafish embryo heart and successfully established an animal model and platform in which to study the electrophysiological mechanism of SCD for human cardiac hypertrophy and diastolic heart failure.

Table. Morphological Phenotypes of Zebrafish Embryos Derived From Fertilized Eggs Injected With Mybpc3-MO

Injection Dose (per Embryo), ng	Injected Embryos	No. of Surviving Embryos* (Survival Rates), %†	Embryos Without Defective Heart Phenotype, %‡	Embryos With Defective Heart Phenotype, %‡
2.0	368	244 (66.3)	156 (63.9)	88 (36.1)
2.5	295	205 (69.5)	128 (62.4)	77 (37.6)
3.0	380	250 (65.8)	134 (53.6)	116 (46.4)
3.5	327	159 (48.6)	93 (58.5	66 (41.5)
4.0	397	126 (31.7)	74 (58.7)	52 (41.3)

MO indicates morpholino; MYBPC, myosin binding protein C.
*Total number of the surviving embryos in triplicate experiments.
†Survival rates indicate the number of surviving embryos among the number of injected embryos.
‡Percentages indicate the number of embryos without or with defective heart phenotype among the numbers of surviving embryos.

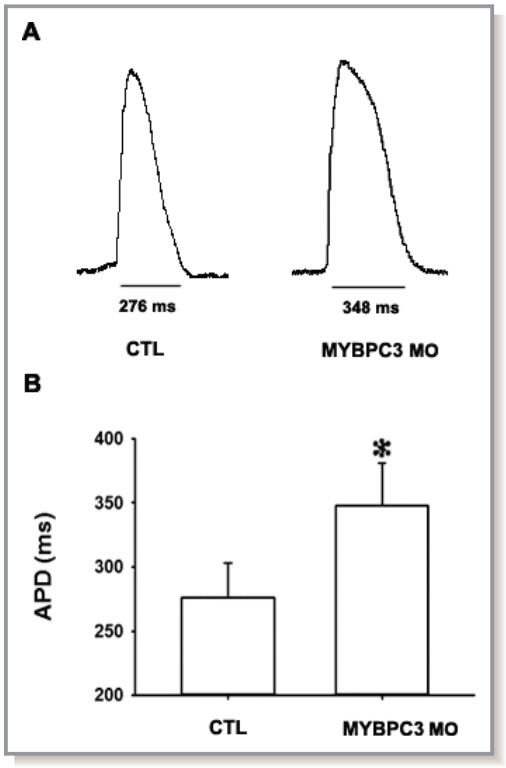

Figure 4. Explanted Mybpc3-MO–injected hearts have longer action potential durations (APDs). A, Representative action potentials of Mybpc3-MO–injected (MYBPC3 MO) and control (CTL) hearts. The MYBP MO heart has a longer APD. B, The mean APD was longer in the MYBPC3 MO hearts than the control (CTL) hearts. *P<0.05 vs controls. MO indicates morpholino; mybpc, myosin binding protein C.

Previous studies have shown that loss of *mybpc3* in mammalian hearts leads to cardiac hypertrophy,[3,4] which is often demonstrated by cardiac imaging, such as echocardiography or magnetic resonance imaging. This kind of imaging modality is not feasible in the embryonic zebrafish heart. However, in the present study, we provided several lines of evidence to demonstrate cardiac hypertrophy in the small embryonic zebrafish heart, such as increased myocardial wall thickness and increased expression of sarcomere protein cmlc2 by nonquantitative measurement.[26,27] Other convincing data to prove the presence of ventricular hypertrophy in our zebrafish model are marked diastolic dysfunction and dilated atrium. It has been shown in humans that left ventricular hypertrophy is often accompanied by ventricular diastolic dysfunction and dilated atrium.[24,25] Therefore, the present zebrafish model of *mybpc3* knockdown may be a good model in which to study the pathophysiology of human cardiac hypertrophy or diastolic dysfunction, such as the electrophysiological abnormalities as demonstrated in the present study. Although there have been several murine models of cardiac hypertrophy,[4,9,10] using zebrafish as a model system provides major advantages of easy genetic manipulation, high throughput, and efficient data profiling. Moreover, accumulating evidence has shown that the electrophysiological phenotypes of zebrafish heart are much closer to those of human heart than are the murine hearts.[10,12]

It has been demonstrated that cardiac ALT, that is, beat-to–beat alternation of cardiac repolarization or APD, is a highly sensitive marker of susceptibility to SCD.[30,34,35] Beat-to-beat alternation of APD, or APD-ALT, produces a repolarization gradient or spatial heterogeneity of refractoriness and facilitates the occurrence of conduction block and the initiation of reentrant arrhythmia. Accumulating evidence has showed that this arrhythmogenic APD-ALT may arise from defective calcium reuptake kinetics and Ca-ALT.[21,30,31] In the present study, we showed that zebrafish hearts with *mybpc3* knockdown displayed defective calcium cycling. Accordingly, in addition to cardiac hypertrophy and diastolic dysfunction, these hearts showed increased susceptibility to Ca-ALT and APD-ALT. Again, these results prove the concept that zebrafish heart could be used as a model system in which to study the molecular mechanism of ventricular arrhythmia or SCD related to cardiac hypertrophy. For example, selective gene manipulation may be performed in the future to test whether hypertrophy-related arrhythmogenic cardiac ALT could be abolished or prevented. Then, this gene may become the target for subsequent drug development to treated hypertrophy-related SCD.

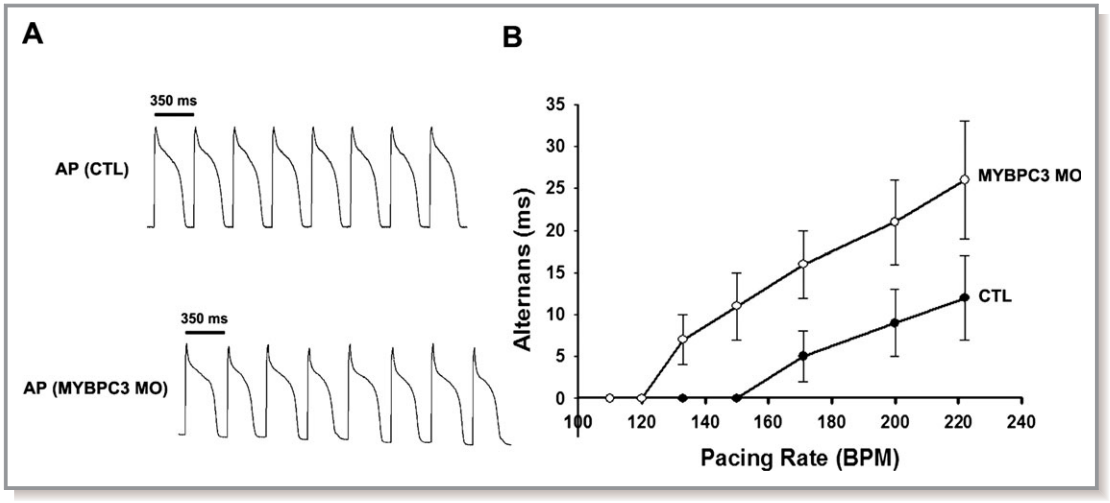

Figure 5. Explanted Mybpc3-MO–injected hearts have an increased susceptibility to action potential duration alternans (APD-ALT). A, Representative action potential tracings at 350 ms pacing cycle length for both Mybpc3-MO–injected (MYBPC3 MO) and control (CTL) hearts are shown. Significant APD alternans is seen in the MYBPC3 MO heart (lower panel), but not in the CTL heart (upper panel). B, Summary data for all experiments demonstrating the relationship of pacing rate (PR) and alternans from CTL and MYBPC3 MO hearts are shown. In MYBPC3 MO hearts, more APD-ALT was observed at each PR tested, with a leftward shift in APD-ALT–to–PR relationship. MO indicates morpholino; mybpc, myosin binding protein C.

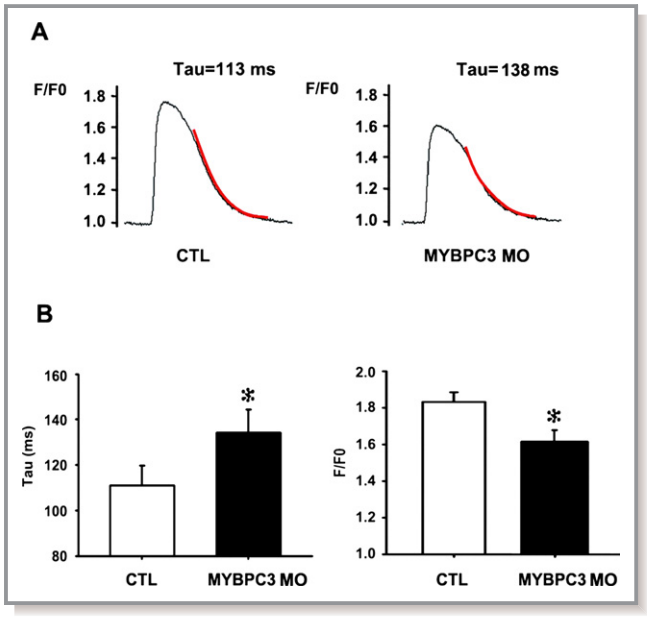

Figure 6. Explanted Mybpc3-MO–injected hearts have a slower calcium reuptake kinetics. A, Representative calcium transients from control (CTL) and Mybpc3-MO–injected (MYBPC3 MO) hearts are shown. Calcium transients were expressed as F/F0 (fluorescence level [F] normalized to diastolic fluorescence level [F0]). The decay portion of the calcium transient (from 30% to 100% of decline phase) was marked as a red curve and was fit to a single exponential function whose time constant, τ, was used to measure Ca^{2+} decay. B, Summary data of τ and calcium transient amplitude in CTL and MYBPC3 MO hearts at a baseline pacing rate (PR) of 120 bpm. The τ was larger in MYBPC3 MO hearts than in CTL hearts, reflecting a slower Ca^{2+} decay rate. The calcium transient amplitude was also significantly smaller in the MYBPC3 MO hearts than in the CTL hearts. *P<0.05 vs controls. MO indicates morpholino; mybpc, myosin binding protein C.

We also first demonstrated that arrhythmogenic cardiac ALT could be induced in the hypertrophic heart, providing the possible electrophysiological mechanism of increased risk of SCD in patients with cardiac hypertrophy.[6,36,37] Our results also implicate the possibility of increased susceptibility to SCD or severe ventricular arrhythmia in patients with diastolic heart failure or HFNEF, which has never been addressed before. Our results also imply that screening of *mybpc3* genetic variation may be one of the strategies for SCD risk stratification in patients with diastolic heart failure or HFNEF. Chen et al[38] also reported a mouse model with conditional knockout of *mbyc3* in the heart. The cardiac phenotypes of this mouse model were very close to those of our zebrafish model, such as cardiac hypertrophy, cardiac diastolic dysfunction, and preserved systolic function. This may be another model in which to study the electrophysiological mechanism of SCD in cardiac hypertrophy or HFNEF. However, no electrophysiological phenotypes had been characterized in this murine cardiac hypertrophy model. As mentioned previously, it is very difficult to study cardiac repolarization in the mouse heart because of the extremely short APD.

Conclusions

We characterized the functional role of *mybpc3* gene in terms of cardiac morphological, mechanical, and electrophysiological phenotypes and established the fundamental role of MYBPC in the mechanism of cardiac hypertrophy, diastolic dysfunction, and arrhythmogenic cardiac ALT. The results of the present study provide the rationale to develop novel

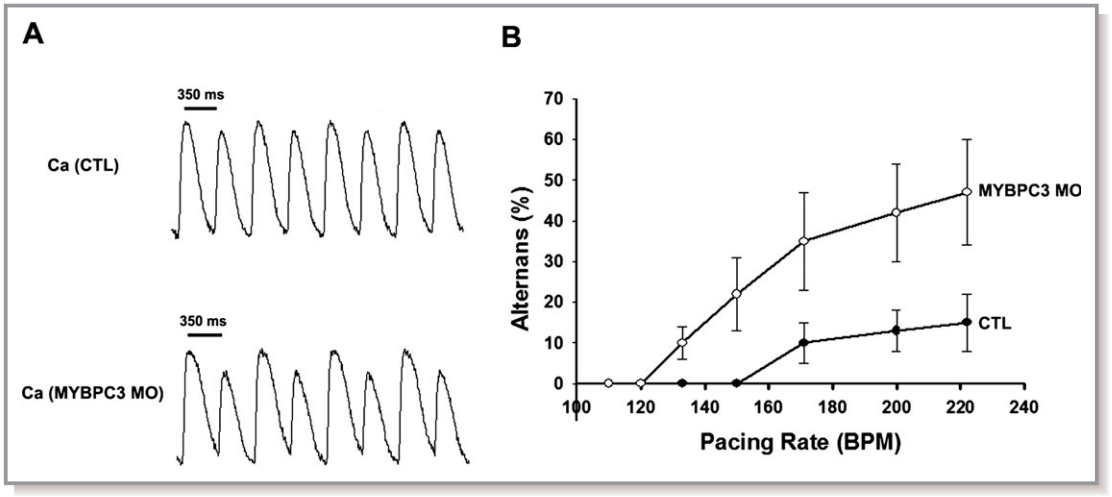

Figure 7. Explanted Mybpc3-MO–injected hearts have an increased susceptibility to calcium transient alternans (Ca-ALT). A, Representative calcium transient tracings at 350 ms pacing cycle length for both Mybpc3-MO–injected (MYBPC3 MO) and control (CTL) hearts are shown. Ca-ALT is much more significant in the MYBPC3 MO heart (lower panel) than in the CTL heart (upper panel). B, Summary data for all experiments demonstrating the relationship of pacing rate (PR) and alternans from CTL and MYBPC3 MO hearts are shown. In MYBPC3 MO hearts, more Ca-ALT was observed at each PR tested, with a leftward shift in Ca-ALT–to–PR relationship.

therapy targeting MYBPC to prevent SCD in cardiac hypertrophy or diastolic heart failure.

Sources of Funding

This work was supported by grants from the National Taiwan University Hospital, Taipei, Taiwan (99-S1283, 99CGN12, 100CGN10, 100-S1650, UN102-052, 102-S2155, 102-P04), the National Science Council of Taiwan (99-2314-B-002 -118-MY3, 101-2314-B-002-181-MY3 and 102-2628-B-002 -035-MY3), and the New Century Health Care Promotion Foundation.

Disclosures

None.

References

1. McClellan G, Kulikovskaya I, Winegrad S. Changes in cardiac contractility related to calcium-mediated changes in phosphorylation of myosin-binding protein c. *Biophys J* . 2001;81:1083–1092.
2. Dhandapany PS, Sadayappan S, Xue Y, Powell GT, Rani DS, Nallari P, Rai TS, Khullar M, Soares P, Bahl A, Tharkan JM, Vaideeswar P, Rathinavel A, Narasimhan C, Ayapati DR, Ayub Q, Mehdi SQ, Oppenheimer S, Richards MB, Price AL, Patterson N, Reich D, Singh L, Tyler-Smith C, Thangaraj K. A common mybpc3 (cardiac myosin binding protein c) variant associated with cardiomyopathies in south asia. *Nat Genet*. 2009;41:187–191.
3. Girolami F, Ho CY, Semsarian C, Baldi M, Will ML, Baldini K, Torricelli F, Yeates L, Cecchi F, Ackerman MJ, Olivotto I. Clinical features and outcome of hypertrophic cardiomyopathy associated with triple sarcomere protein gene mutations. *J Am Coll Cardiol*. 2010;55:1444–1453.
4. Harris SP, Bartley CR, Hacker TA, McDonald KS, Douglas PS, Greaser ML, Powers PA, Moss RL. Hypertrophic cardiomyopathy in cardiac myosin binding protein-c knockout mice. *Circ Res*. 2002;90:594–601.
5. Wu CK, Huang YT, Lee JK, Chiang LT, Chiang FT, Huang SW, Lin JL, Tseng CD, Chen YH, Tsai CT. Cardiac myosin binding protein C and MAP-kinase activating death domain-containing gene polymorphisms and diastolic heart failure. *PLoS ONE*. 2012;7:e35242.
6. Haider AW, Larson MG, Benjamin EJ, Levy D. Increased left ventricular mass and hypertrophy are associated with increased risk for sudden death. *J Am Coll Cardiol*. 1998;32:1454–1459.
7. Kannel WB, Abbott RD. A prognostic comparison of asymptomatic left ventricular hypertrophy and unrecognized myocardial infarction: the Framingham study. *Am Heart J*. 1986;111:391–397.
8. Harzheim D, Movassagh M, Foo RS, Ritter O, Tashfeen A, Conway SJ, Bootman MD, Roderick HL. Increased InsP3Rs in the junctional sarcoplasmic reticulum augment Ca2+ transients and arrhythmias associated with cardiac hypertrophy. *Proc Natl Acad Sci USA*. 2009;106:11406–11411.
9. von Lueder TG, Gravning J, How OJ, Vinge LE, Ahmed MS, Krobert KA, Levy FO, Larsen TS, Smiseth OA, Aasum E, Attramadal H. Cardiomyocyte-restricted inhibition of G protein-coupled receptor kinase-3 attenuates cardiac dysfunction after chronic pressure overload. *Am J Physiol Heart Circ Physiol*. 2012;303:H66–H74.
10. Arnaout R, Ferrer T, Huisken J, Spitzer K, Stainier DY, Tristani-Firouzi M, Chi NC. Zebrafish model for human long QT syndrome. *Proc Natl Acad Sci USA*. 2007;104:11316–11321.
11. Lin JL, Lai LP, Lin CS, Du CC, Wu TJ, Chen SP, Lee WC, Yang PC, Tseng YZ, Lien WP, Huang SK. Electrophysiological mapping and histological examinations of the swine atrium with sustained (> or =24 h) atrial fibrillation: a suitable animal model for studying human atrial fibrillation. *Cardiology*. 2003;99:78–84.
12. Tsai CT, Wu CK, Chiang FT, Tseng CD, Lee JK, Yu CC, Wang YC, Lai LP, Lin JL, Hwang JJ. In-vitro recording of adult zebrafish heart electrocardiogram – a platform for pharmacological testing. *Clin Chim Acta*. 2011;412:1963–1967.
13. Chen YH, Lee WC, Liu CF, Tsai HJ. Molecular structure, dynamic expression and promoter analysis of zebrafish (*Danio rerio*) *myf*-5 gene. *Genesis*. 2001;29:22–35.
14. Chen YH, Lin YT, Lee GH. Novel and unexpected functions of zebrafish CCAAT box binding transcription factor (NF-Y) B subunit during cartilages development. *Bone*. 2009;44:777–784.
15. Matthews M, Varga ZM. Anesthesia and euthanasia in zebrafish. *ILAR J*. 2012;53:192–204.
16. Kimmel CB, Ballard WW, Kimmel SR, Ullmann B, Schilling TF. Stages of embryonic development of the zebrafish. *Dev Dyn*. 1995;203:253–310.
17. Huang CJ, Tu CT, Hsiao CD, Hsieh FJ, Tsai HJ. Germ-line transmission of a myocardium-specific GFP transgene reveals critical regulatory elements in the cardiac myosin light chain 2 promoter of zebrafish. *Dev Dyn*. 2003; 228:30–40.
18. Shin JT, Ward JE, Collins PA, Dai M, Semigran HL, Semigran MJ, Seldin DC. Overexpression of human amyloidogenic light chains causes heart failure in embryonic zebrafish: a preliminary report. *Amyloid*. 2012;19:191–196.

19. Denvir MA, Tucker CS, Mullins JJ. Systolic and diastolic ventricular function in zebrafish embryos: influence of norepenephrine, MS-222 and temperature. *BMC Biotechnol*. 2008;8:21.
20. Tsai CT, Wang DL, Chen WP, Hwang JJ, Hsieh CS, Hsu KL, Tseng CD, Lai LP, Tseng YZ, Chiang FT, Lin JL. Angiotensin II increases expression of alpha1C subunit of L-type calcium channel through a reactive oxygen species and cAMP response element-binding protein-dependent pathway in HL-1 myocytes. *Circ Res*. 2007;100:1476–1485.
21. Tsai CT, Chiang FT, Tseng CD, Yu CC, Wang YC, Lai LP, Hwang JJ, Lin JL. Mechanical stretch of atrial myocyte monolayer decreases sarcoplasmic reticulum calcium adenosine triphosphatase expression and increases susceptibility to repolarization alternans. *J Am Coll Cardiol*. 2011;58:2106–2115.
22. Wu CK, Lee JK, Chiang FT, Yang CH, Huang SW, Hwang JJ, Lin JL, Tseng CD, Chen JJ, Tsai CT. Plasma levels of tumor necrosis factor-α and interleukin-6 are associated with diastolic heart failure through downregulation of sarcoplasmic reticulum Ca2+ ATPase. *Crit Care Med*. 2011;39:984–992.
23. Laurita KR, Katra R, Wible B, Wan X, Koo MH. Transmural heterogeneity of calcium handling in canine. *Circ Res*. 2003;92:668–675.
24. Cacciapuoti F, Scognamiglio A, Paoli VD, Romano C, Cacciapuoti F. Left atrial volume index as indicator of left ventricular diastolic dysfunction: comparation between left atrial volume index and tissue myocardial performance index. *J Cardiovasc Ultrasound*. 2012;20:25–29.
25. Rossi A, Cicoira M, Florea VG, Golia G, Florea ND, Khan AA, Murray ST, Nguyen JT, O'Callaghan P, Anand IS, Coats A, Zardini P, Vassanelli C, Henein M. Chronic heart failure with preserved left ventricular ejection fraction: diagnostic and prognostic value of left atrial size. *Int J Cardiol*. 2006;110:386–392.
26. Karagiannis TC, Lin AJ, Ververis K, Chang L, Tang MM, Okabe J, El-Osta A. Trichostatin A accentuates doxorubicin-induced hypertrophy in cardiac myocytes. *Aging (Albany NY)*. 2010;2:659–668.
27. Garciarena CD, Pinilla OA, Nolly MB, Laguens RP, Escudero EM, Cingolani HE, Ennis IL. Endurance training in the spontaneously hypertensive rat: conversion of pathological into physiological cardiac hypertrophy. *Hypertension*. 2009;53:708–714.
28. Beuckelmann DJ, Näbauer M, Erdmann E. Intracellular calcium handling in isolated ventricular myocytes from patients with terminal heart failure. *Circulation*. 1992;85:1046–1055.
29. Richard S, Leclercq F, Lemaire S, Piot C, Nargeot J. Ca2+ currents in compensated hypertrophy and heart failure. *Cardiovasc Res*. 1998;37:300–311.
30. Pastore JM, Girouard SD, Laurita KR, Akar FG, Rosenbaum DS. Mechanism linking T-wave alternans to the genesis of cardiac fibrillation. *Circulation*. 1999;99:1385–1394.
31. Pruvot EJ, Katra RP, Rosenbaum DS, Laurita KR. Role of calcium cycling versus restitution in the mechanism of repolarization alternans. *Circ Res*. 2004;94:1083–1090.
32. Wilson LD, Jeyaraj D, Wan X, Hoeker GS, Said TH, Gittinger M, Laurita KR, Rosenbaum DS. Heart failure enhances susceptibility to arrhythmogenic cardiac alternans. *Heart Rhythm*. 2009;6:251–259.
33. Norton N, Li D, Rieder MJ, Siegfried JD, Rampersaud E, Züchner S, Mangos S, Gonzalez-Quintana J, Wang L, McGee S, Reiser J, Martin E, Nickerson DA, Hershberger RE. Genome-wide studies of copy number variation and exome sequencing identify rare variants in BAG3 as a cause of dilated cardiomyopathy. *Am J Hum Genet*. 2011;88:273–282.
34. Verrier RL, Nearing BD, La Rovere MT, Pinna GD, Mittleman MA, Bigger JTJr, . Schwartz PJ, ATRAMI Investigators. Ambulatory electrocardiogram-based tracking of T wave alternans in postmyocardial infarction patients to assess risk of cardiac arrest or arrhythmic death. *J Cardiovasc Electrophysiol*. 2003;14:705–711.
35. El-Sherif N, Caref EB, Yin H, Restivo M. The electrophysiological mechanism of ventricular arrhythmias in the long QT syndrome – Tridimensional mapping of activation and recovery patterns. *Circ Res*. 1996;79:474–492.
36. Chiang BN, Perlman LV, Fulton M, Ostrander LDJ, Epstein FH. Predisposing factors in sudden cardiac death in Tecumseh, Michigan: a prospective study. *Circulation*. 1970;41:31–37.
37. Kannel WB, Schatzkin A. Sudden death: lessons from subsets in population studies. *J Am Coll Cardiol*. 1985;5:141B–149B.
38. Chen PP, Patel JR, Powers PA, Fitzsimons DP, Moss RL. Dissociation of structural and functional phenotypes in cardiac myosin-binding protein C conditional knockout mice. *Circulation*. 2012;126:1194–1205.